International Journal of Innovative Technologies
WWW.IJITECH.ORG
ISSN 2321-8665
Vol.06,Issue.01,
January-2018,
Pages:0017-0024

Stability Improvement of DFIG System

C. NAGAMANI[1], K. VIJAYA KAMAL[2], G. VENKATA SURESH BABU[3]
[1]PG Scholar, Dept of EEE(EPS), SITS, Kadapa, Andhrapradesh, India.
[2]Assistant Professor, Dept of EEE, SITS, Kadapa, Andhrapradesh, India.
[3]Associate Professor & HOD, Dept of EEE, SITS, Kadapa, Andhrapradesh, India.

Abstract: In an electric power grid that has a high penetration level of wind, the power fluctuation of a large-scale wind power plant (WPP) caused by varying wind speeds deteriorates the system frequency regulation. This paper proposes a disturbance-adaptive short term frequency support scheme of a doubly fed induction generator (DFIG) that can improve the frequency-supporting capability while ensuring stable operation. The proposed scheme employs an additional control loop relying on the system frequency deviation that operates in combination with the maximum power point tracking control loop. To improve the power-smoothing capability while preventing over-deceleration of the rotor speed, the gain of the additional loop is modified with the rotor speed and frequency deviation. The gain is set to be high if the rotor speed and/or frequency deviation is large.The simulation results demonstrate that the proposed scheme significantly lessens the output power fluctuation of a WPP under various scenarios by modifying the gain with the rotor speed and frequency deviation, and thereby it can regulate the frequency deviation within a narrow range.

Keywords: Adaptive Gain, Disturbance-Adaptive, Frequency Nadir (FN), Stable Operation, Short-Term Frequency Support (STFS).

I. INTRODUCTION

During the last decade, renewable energy has developed dramatically worldwide due to subsidies and tax allowances set for private investors. In Europe, the feed-in tariff, which mandates the purchase of energy from renewable sources at set prices, is the dominant promotion policy for renewables. The United States has put forth a tax credit policy with a renewable portfolio standard until 2012 to aid in the integration of renewable generation. Large-scale integration of wind power, however, gives rise to new challenges for the electric grid. The inflexible and intermittent nature of wind resources adds complexity to the operations of a power system; yet reliability, stability and security requirements must be maintained. Thus, as penetration levels increase to the extent that conventional generators are partially displaced, it becomes necessary to ensure that connected wind power plants will contribute to the smooth operation of the power system in a similar manner as conventional generators do. Wind variability dictates that a wind power plant is a source of energy, with very limited capacity value. Fluctuations in generated power result in complications in terms of line congestion, market prices, frequency regulation and power system stability. These phenomena are particularly pronounced in isolated grids with a high wind power penetration. In the frame ranging from a few seconds to minutes, wind power is perturbed by gusts that can affect frequency regulation of the overall power system.

These short-term fluctuations are characterized by their frequency spectra. The impacts of minute-to-minute variations of wind power on power system operation were studied, where wind power variations are decomposed into a slow moving average, a fast fluctuating part, and ramp event components to assess the influence of each component on system operation. Most recent grid codes impose requirements on active power regulation capabilities of wind farms. From the point of view of the system operator (SO), the ability to control active power is important during normal operation to avoid frequency deviations, and during transient fault situations to guarantee transient and voltage stability. Within the primarily available active power from the wind, output power can be regulated to a specific value1 or to bear a fixed relationship to the available power, such as maintaining a specified reserve either in megawatts or as a percentage of the available power. Modern variable speed wind turbine generators are capable of fast decoupled active and reactive power control, which makes possible several valuable ancillary services. Contribution to frequency regulation can be achieved by modulating a fraction of the available power in the wind. Control schemes that allow WTGs to participate in frequency support have been pursued along several directions, as shown in Figure1.

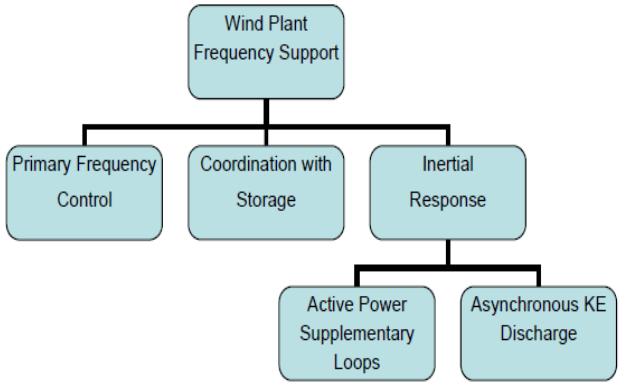

Fig1. Research sub-areas addressing frequency support from wind power plants.

Primary frequency control from wind plants consists of operating the individual generators at de-loaded levels under normal conditions, thus maintaining a generation margin that can be utilized in the event of under-frequency. This is usually done by controlling the blade pitch angle to adjust generation. Although this would potentially provide a more flexible, longer-term frequency support, it has undesired economical implications as it reduces annual production. This mode of operation, however, may become necessary as future grid code provisions get tighter on wind power plants. Incorporation of storage has also been investigated to improve frequency control for systems with high wind power penetration, including battery systems, and superconducting magnetic energy storage systems. Coordination with other distributed generation has also been researched. Inertial response from wind power plants has been researched in two approaches. In the first approach, supplementary loops have been incorporated into the speed controller of individual WTGs to release the kinetic energy stored in the turbine blades. An additional power component, proportional to the frequency deviation or derivative, is added to the power reference set by the maximum power tracking (MPT) loop to couple the WTG to grid. Thus, the inertial response is exhibited by each grid-connected WTG independent of the other generators in the wind plant. Additional requirements include the limitation of the ramp rate of output power.

In some codes, frequency response is requested for both over-frequency and under frequency deviations. In the latter case, the wind farm might have to operate with a power reserve when frequency is in its normal operating range, which has undesirable economic implications as it reduces annual production levels. Thus, a dynamic gain–based STFS scheme has been suggested that uses the Δf loop only, but it changes the control gain based on df/dt. This scheme can improve the FN and maximum df/dt by releasing a large amount of KE during the initial stage of an event. In this scheme, a shaping function, which relates the gain of the Δf loop to df/dt, is defined for a rotor speed prior to an event; in addition, the gain of the Δf loop is modified with df/dt only. Thus, OD might occur if a subsequent event occurs and/or the wind speed decreases while stabilizing the frequency. This paper proposes an adaptive STFS scheme of a DFIG that can improve the FN and maximum df/dt while ensuring stable operation. In the proposed scheme, the output of the Δf loop is determined as the product of the Δf and adaptive gain, which is modified with df/dt and the rotor speed. The adaptive gain is set to be high during the early stage of a disturbance, when the df/dt and rotor speed are high. Until the FN, the gain decreases with df/dt and rotor speed. After the FN, the gain decreases only with the rotor speed. The performance of the proposed scheme was investigated under various wind conditions and disturbances using an EMTP-RV simulator in a power grid consisting of steam turbine generators, which have a low ramping capability, particularly if the wind speed decreases during the STFS and a consecutive event occurs.

II. SYSTEM MODELING

Frequency is an indicator of the balance between generation and load. As frequency is common throughout the system, a change in active power demand or supply at one point is reflected throughout the system by a change in frequency. For safe and reliable operation, the frequency should remain nearly constant. This is done by adjusting generation in real time to match load deviations. Tight control of frequency ensures consistency of the speed of induction and synchronous motors. A considerable drop in frequency can result in high magnetizing currents in induction motors and transformers. In addition, old grid-connected generators may still use the system frequency as the time standard for their electric clocks. In a generation deficit situation, such as a sudden load increase, tripping of a large generator, or a fault on a major tie line, the frequency and its rate of change must be maintained above a grid-specific threshold. Otherwise, automatic under-frequency protection relays will be activated, thus affecting customers. Traditionally, wind plants do not participate in maintaining the system frequency under control. Hence, WTGs do not increase or decrease their production when frequency falls or rises, respectively, which means they do not contribute to grid inertia. In countries where significant wind energy penetration is experienced or expected, grid operators are concerned about frequency security as system inertia is decreasing. This effect is mainly noticeable in small or isolated systems, such as those of UK, Ireland or Hawaii. Other traditionally strong systems are behaving like isolated grids with respect to frequency regulation when their interconnections with neighboring systems are replaced by dc links.

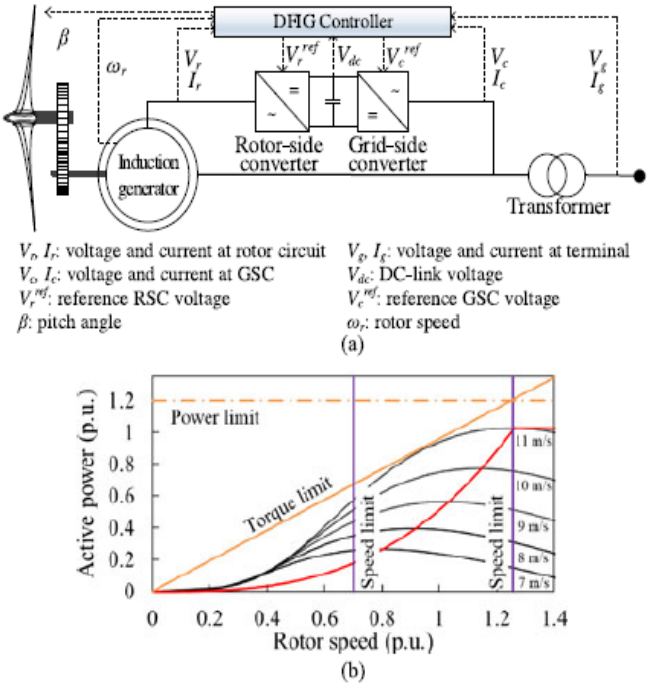

Fig.2. Configuration and power characteristics of a DFIG. (a)Configuration of a DFIG. (b) Power characteristics and torque, power, and rotor speed limits.

Several studies have evaluated the impact of large-scale wind power integration on frequency control. In Lalor *et al.* examined the amendments needed in reserve policies of the Irish grid to cope with the deterioration of frequency response as conventional generators are replaced by DFIG-based WTGs. Pearmine *et al.* developed a process to optimize the primary response requirements while maintaining statutory limits on frequency deviation; the method was validated against historic generation loss events. In Luo *et al.* proposed a transfer function-based method to estimate the frequency deviation caused by fluctuations in wind power. Later, they estimate the allowable level of wind power penetration as limited by frequency deviation. Remedies for the deterioration in frequency response caused by large-scale integration of variable-speed wind plants have been pursued along two main directions. In the first direction, traditional control of conventional plants is modified taking into consideration the wind generation. For example, a new governor for conventional plants was designed in to attenuate frequency deviation caused by wind power fluctuations. In the second direction, researchers have looked into methods for implementing primary control in wind generation itself to support the grid and reduce reserve costs. Fig2 shows a typical configuration and power characteristics of a DFIG, which includes a mechanical power model, two mass shaft model, back-to-back converters, and DFIG controller. A rotor-side converter (RSC) and grid-side converter (GSC) comprise the DFIG controller. The RSC controls the active power and reactive power injected into a system; the GSC is used to maintain the DC-link voltage and control the terminal voltage. Further, a pitch-angle controller is used to prevent the rotor speed from exceeding the maximum operating limit. In addition, to obtain the realistic results, this paper considers the power, torque, and rate limits.

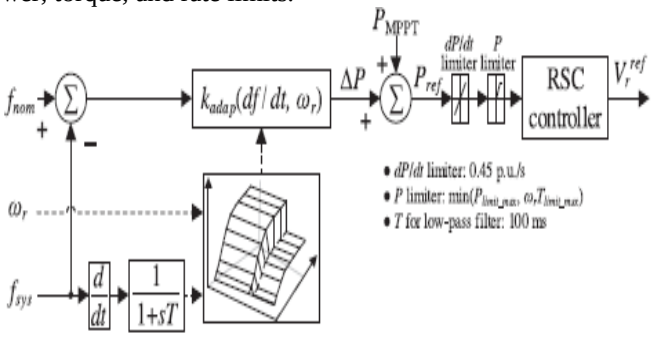

Fig.3. Proposed STFS scheme associated with the adaptive gain.

The proposed adaptive STFS scheme aims to improve the FN and maximum *df/dt* while ensuring stable operation of a DFIG under disturbances. To achieve these objectives, the proposed scheme uses the Δ*f* loop operating in association with the MPPT control loop, as shown in Fig3. In this paper, the system frequency for STFS is obtained in the DFIG controller from the measured voltage of an aggregated WPP terminal using a phase-locked loop proposed. The performance of the STFS schemes is affected by the wind conditions including turbulence,system inertia, and capacity of the tripped generator.

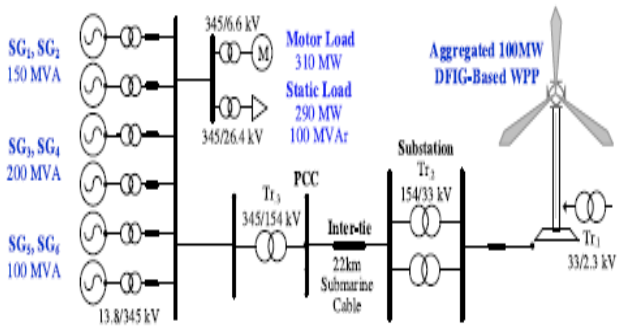

Fig.4. Model System.

III. SIMULATION RESULTS

To validate the performance of the STFS schemes, the system shown in modeled using an Matlab/Simulink. The STFS capability of a DFIG critically depends on the stored KE, which is directly related to the wind speed. In addition, the capacity of the tripped generator impacts the frequency-supporting capability of a DFIG. Thus, this section investigates the performance of STFS schemes for wind speeds of 10 m/s and 8 m/s with different generator trips.

CASE-1: Wind Speed of 10 m/s, 80-MW SG Trip

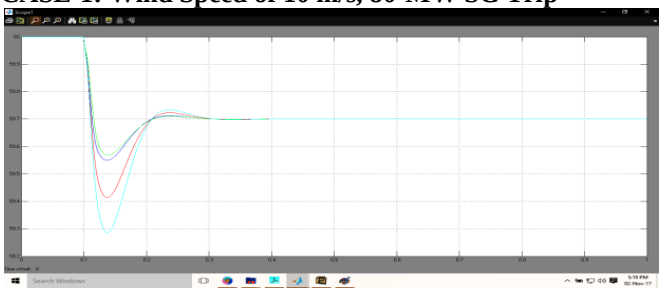

(a)

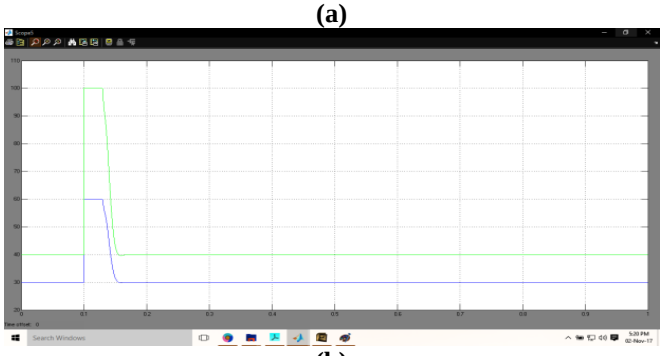

(b)

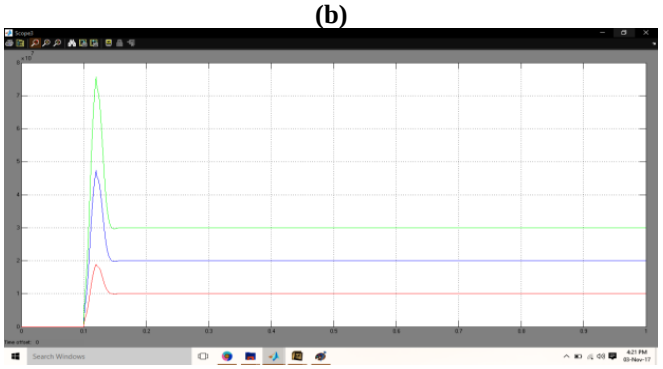

(c)

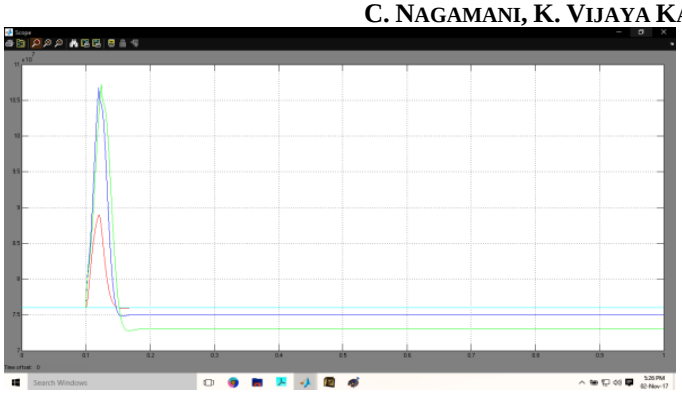

(d)

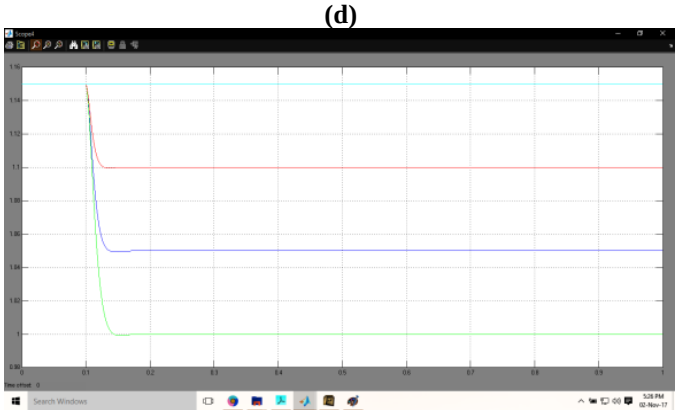

(e)

Fig.5. Results for Case 1. (a) System frequency. (b) Gain in Scheme #2 and the proposed scheme. (c) ΔP. (d) P_{WPP}. (e) Rotor speed.

As a disturbance, SG5 supplying 80 MW prior to a disturbance in the model system is tripped at 0.1 s. The FN of Scheme #2 is slightly higher than that of the proposed scheme. Moreover, the maximum df/dt of Scheme #2 is the smallest. This is because Scheme #2 releases a larger amount of KE during the early stage of an event than Scheme #1 and the proposed scheme (see Fig. 5(d)); thus, after an event, less KE in Scheme #2 is left than in the proposed scheme (see Fig. 5(e)). As shown in Fig. 5(b), during the initial stage of an event, kadap , which varies with df/dt and ωr, has a large value; because the magnitude of df/dt is large and ωr is high. It remains at almost 60 and then decreases as the magnitude of df/dt and ωr decrease. After the frequency rebound, kadap, which is smaller than that in Scheme #2 but larger than that in Scheme #1. This is because ωr converges (see Figs. 5(e) and 5(a)). Note that the gain in Scheme #2 is larger than that in the proposed scheme and thus ΔP in Scheme #2 is larger. However, the output power in Scheme #2 during the initial stage of an event is similar to that of the proposed scheme because the output power is limited by the torque limit (see Fig. 5(d)). Because after the frequency rebound, the proposed scheme reduces the output power faster than Scheme #2, ωr in the proposed scheme converges to a value higher than it does in Scheme #2 (see Fig. 5(e)). This helps a DFIG keep more KE for a subsequent disturbance and ensure stable operation; in addition, it helps ωr quickly return to the optimal value prior to an event.

CASE-2: Wind Speed of 8 m/s, 110-MW SG Trip

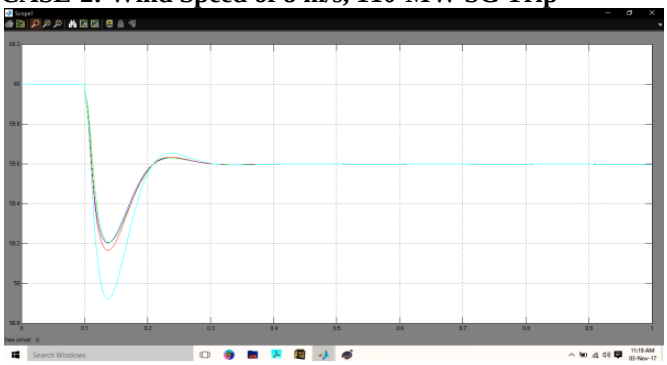

(a)

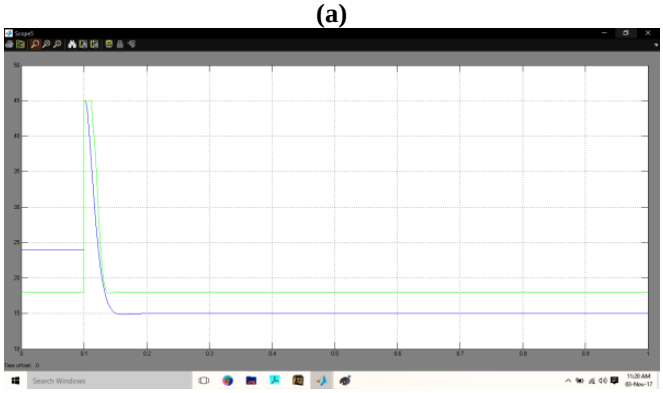

(b)

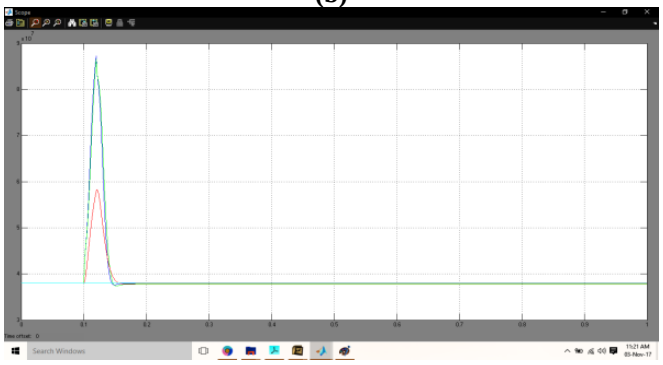

(c)

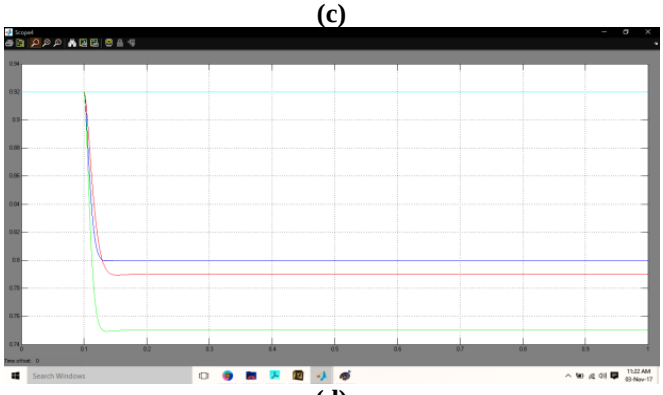

(d)

Fig.6: Results for Case 2. (a) System frequency. (b) Gain in Scheme #2 and the proposed scheme. (c) P_{WPP}. (d) Rotor speed.

In this case, the wind speed is smaller than it is in Case 1; thus, ωr at the beginning of a disturbance is 0.92 p.u., which is smaller. Because the size of a disturbance is larger than it is

in Case 1, the maximum df/dt for "no STFS" is −0.646 Hz/s, which is 1.45 times larger. In addition, the FN is 58.938 Hz, which is lower. As in Case 1, the FN in Scheme #2 is the highest and the maximum df/dt is the smallest. However, in this case, the FN and maximum df/dt in the proposed scheme are similar to those in Scheme #2. kadap , which remains 23.8 prior to an event, reaches 45.5 at the beginning of a disturbance; this value is smaller than it is in Case 1, because ωr is smaller but the maximum df/dt is larger. In this case, when the frequency is settled, kadap converges to 14.7, which is smaller than those of Scheme #1 and Scheme #2 (see Figs. 6(b) and 6(a)). In this case, the proposed scheme reduces the output power faster than Scheme #1 and Scheme #2, thus ωr in the proposed scheme converges to a value higher than it does in Scheme #1 and Scheme #2 (see Figs. 6(d)). The results of the two cases indicate that the proposed scheme can support the frequency during a disturbance while ensuring stable operation of a DFIG irrespective of wind conditions and the sizes of disturbances.

CASE-3: Wind Speed of 10 m/s, 80-MW SG Trip and a Subsequent 100-MW SG Trip

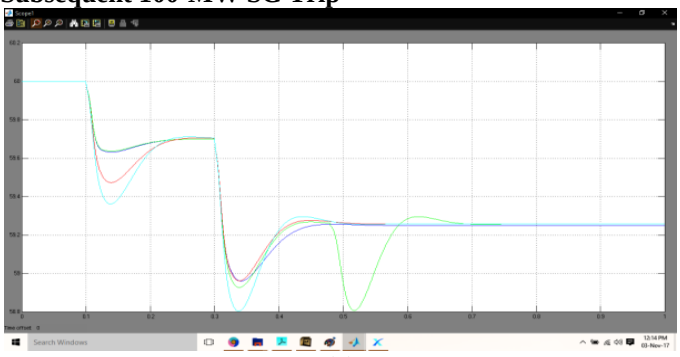

(a)

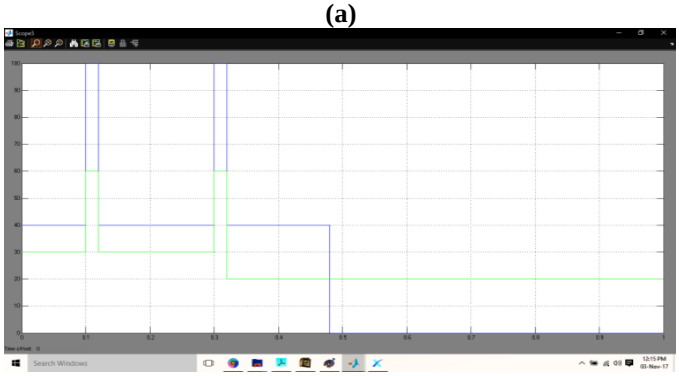

(b)

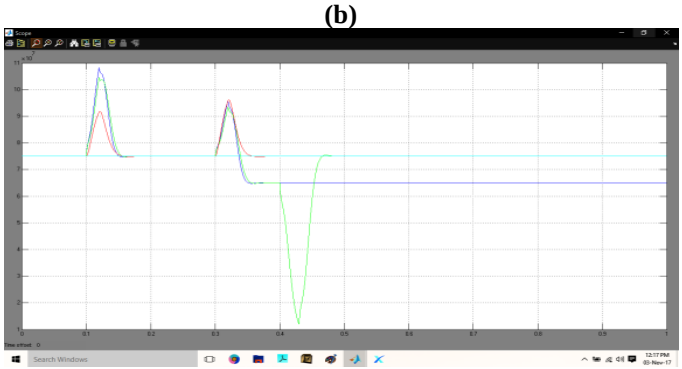

(c)

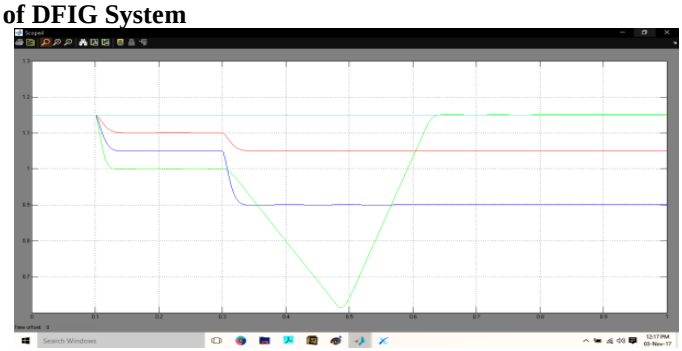

(d)

Fig.7. Results for Case 3. (a) System frequency. (b) Gain in Scheme #2 and the proposed scheme. (c) P_{WPP}. (d) Rotor speed.

Figure 7 show the results for Case 3, which is identical to Case 1 except for the subsequent disturbance at 0.3 s. Thus, the results before 0.3 s in Case 3 are the same as they are in Case 1. When a subsequent trip occurs at 0.3 s, kadap increases up to 56.6, which is smaller than that at the instant of the first disturbance. This is because ωr at the instant of the subsequent trip is 1.04 p.u., which is lower than that at the instant of the first disturbance. Afterward, kadap keeps decreasing with df/dt and ωr , as shown in Fig. 7(b); it converges to 22.8 when the frequency is settled. From 0.1 s to 0.3 s, the proposed scheme reduces the output power slightly faster than Scheme #2 as in Case 1; however, after 0.3 s, the proposed scheme reduces the output power much faster than it does for the first disturbance. Thus, as shown in Fig. 7(d), the proposed scheme successfully prevents OD; in contrast, ωr in Scheme #2 reaches ωmin at 87.6 s, inwhich Scheme #2 is disabled, and thenPref is switched to PMPPT (see Fig. 7(c)). This abrupt change in Pref causes a significant SFD, as shown in Fig. 7(a). As shown in Table IV, the maximum df/dt in the proposed scheme after the second disturbance is the smallest. As in Case 1, the first FN in Scheme #2 is higher than it is in the proposed scheme.

However, the second FN after the subsequent trip in Scheme #2 is lower than that in the proposed scheme by 0.02 Hz. In addition, the third FN in Scheme #2 reaches 58.731 Hz, which is lower than the second FN in Scheme #1. For 7.1 s after the second disturbance, theWPP output power of the proposed scheme is slightly larger than that of Scheme #2 (see Fig. 7(c)). This is because during this period, ωr in Scheme #2 is smaller than that in the proposed scheme; the WPP output power in Scheme #2 and proposed schemes is limited by the torque limit, but the torque limit of Scheme #2 is smaller than that of the proposed scheme because ωr is smaller. As a result of STFS, the stored KE in a WTG decreases. When the frequency is settled, it can be eventually restored to the nominal value in association with automatic generation control. However, if a subsequent event occurs before the frequency is not returned, the performance of the STFS schemes can be affected because of less stored KE. Thus, this section investigates the performance of the STFS for Case 1 and Case 2 followed by a subsequent event. As mentioned in the previous section, the performance of the

STFS is critically dependent on the stored KE, which can be decreased as a result of the frequency-supporting capability and/or because of a decrease in the wind speed. Thus, this section describes the investigation results for a case in which the wind speed decreases from 10 m/s to 7.5 m/s for 1 s at the beginning of a disturbance.

CASE-4: Wind Speed of 8 m/s, 110-MW Generator Trip and a Subsequent 110-MW SG Trip

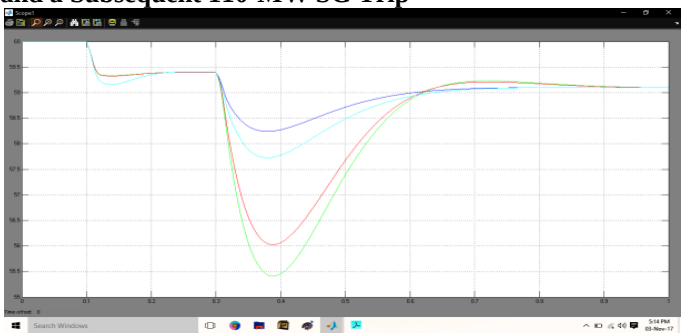

(a)

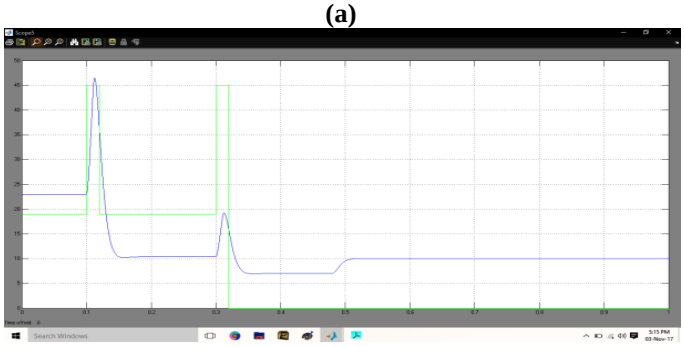

(b)

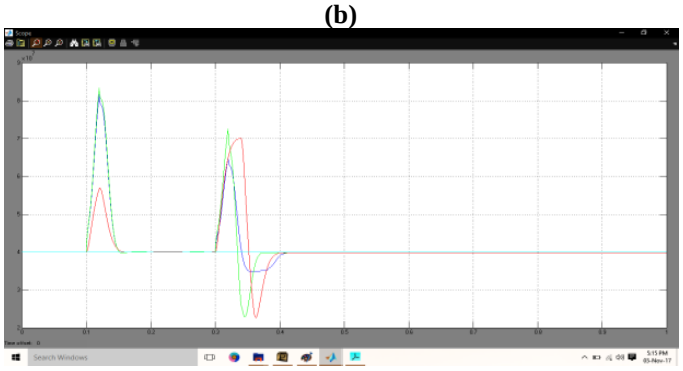

(c)

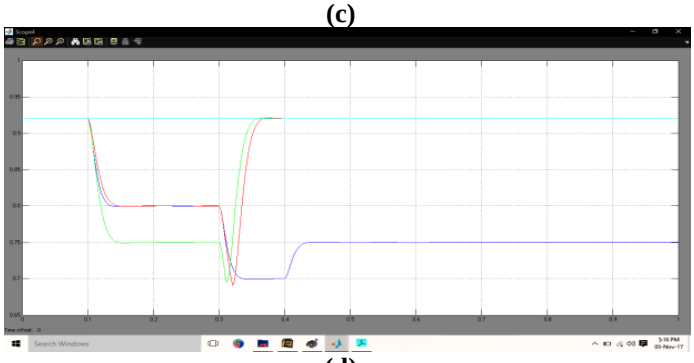

(d)

Fig.8. Results for Case 4. (a) System frequency. (b) Gain in Scheme #2 and the proposed scheme. (c) P_{WPP}. (d) Rotor speed.

Figure 8 shows the results for Case 4, which is identical to Case 2 except for the subsequent disturbance at 0.3 s. As in Case 3, for the second disturbance, kadap increases up to 23.3; however, unlike Case 3 this value is much smaller than that at the instant of the first disturbance. Afterward, kadap keeps decreasing with df/dt and ωr and converges to 9.1. Unlike Case 2, ωr in Scheme #2 reaches ωmin at 0.316 s; further, even in Scheme #1, ωr reaches ωmin at 0.326 s, in which Scheme #1 is also disabled. As a result, the second FN in Scheme #1 and Scheme #2 become significant and lower than it is in the case with "no STFS" (see Fig8(a)). However, the proposed scheme successfully prevents ωr from reaching ωmin. The results in the previous two cases demonstrate that the proposed scheme can arrest the frequency dip without causing ODs by adaptively modifying the control gain even when a subsequent disturbance occurs.

CASE-5: Wind Speed Reduction from 10 m/s to 7.5 m/s for 1 s with an 80-MW Generator Trip

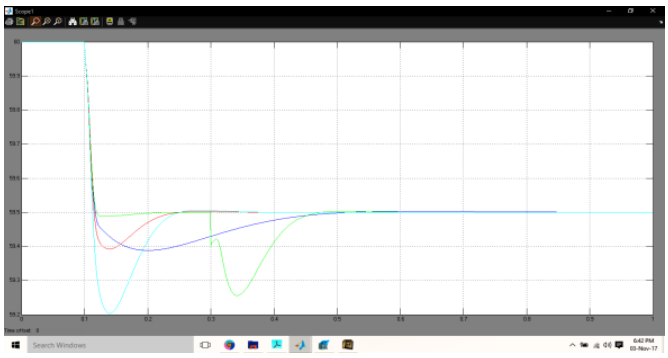

(a)

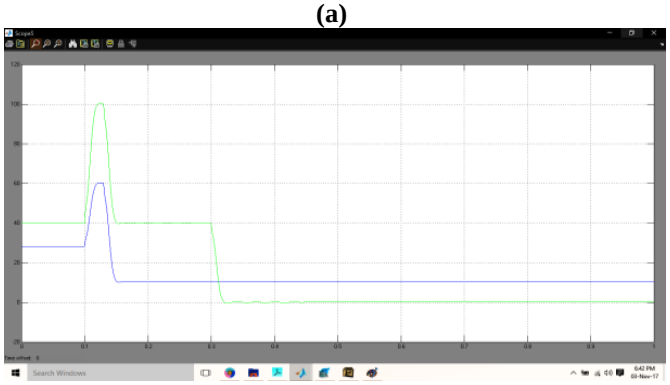

(b)

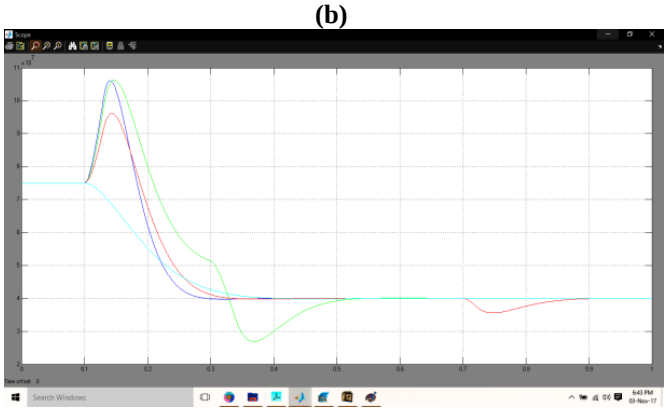

(c)

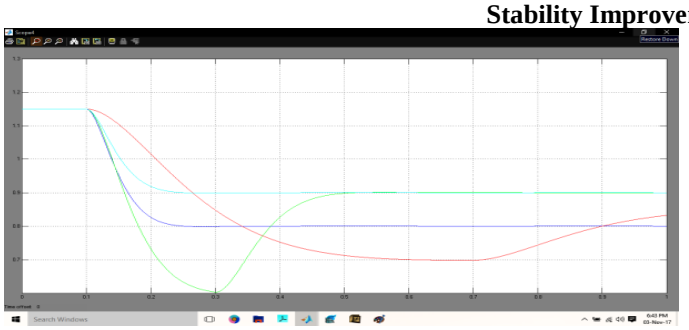

(d)

Fig.9. Results for Case 5. (c) Gain in Scheme #2 and the proposed scheme. (a) Wind speed. (b) System frequency. (c) Gain in Scheme #2 and the proposed scheme. (d) P_{WPP}. (e) Rotor speed.

Figure 9 show the results for Case 5, which is identical to Case 1 except for the decrease in the wind speed from 10 m/s to 7.5 m/s at the onset of a disturbance. Thus, during the early stage of an event, kadap is similar to that in Case 1. However, because the wind speed abruptly decreases for a short interval, ωr promptly decreases. Thus, Scheme #1 and Scheme #2 reach ωmin at 0.74 s and 0.36 s, respectively, when the two STFS schemes are disabled. Consequently, a significant SFD for Scheme #2 and a less significant SFD for Scheme #1 occur. This is because Scheme #2 causes a larger power deficit at the instant of the disablement, whereas Scheme #1 causes a smaller power deficit. However, the proposed scheme modifies kadap with df/dt and ωr, as shown in Fig. 9(c), and thus it prevents ωr from reaching ωmin, thereby causing no SFD. As in Case 1, the first FN for Scheme #2 is the highest; however, an SFD occurs because of the significant wind speed reduction. The FN for the proposed scheme is 59.370 Hz, which is lower than the first FN for Scheme #2 and higher than the second FN for Scheme #2. In this case, after the FN, kadap keeps decreasing with the decreasing ωr and converges to 10.5 when the frequency is settled; this value is 66% of the gain of Scheme #1. Thus, until the FN, the output power in Scheme #2 is the largest, but after the FN, the output power in the proposed scheme significantly decreases with ωr. In addition, the FN in the proposed scheme is 59.370 Hz, which is higher than the lowest FNs in Scheme #1 and Scheme #2. The above results clearly demonstrate that the proposed scheme ensures no OD by modifying the control gain with ωr even when the wind speed promptly decreases at the beginning of a disturbance. Further, it can improve the frequency supporting capability of a DFIG even in this case.

CASE 6- Wind Speed Reduction from 10 m/s to 7.5 m/s with an 80-MW SG Trip Followed by an 110-MW SG Trip

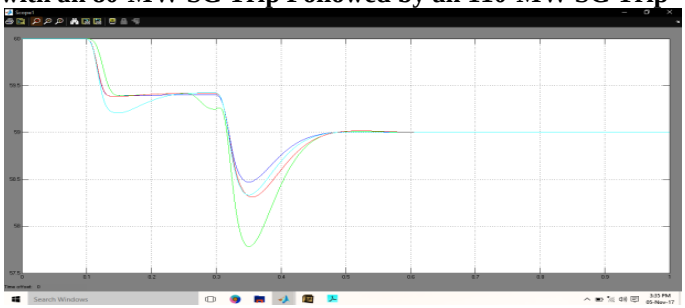

(a)

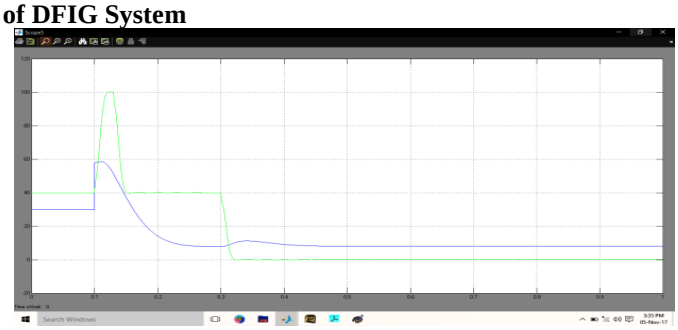

(b)

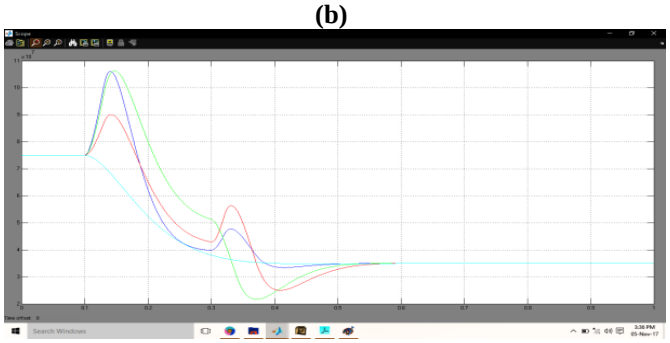

(c)

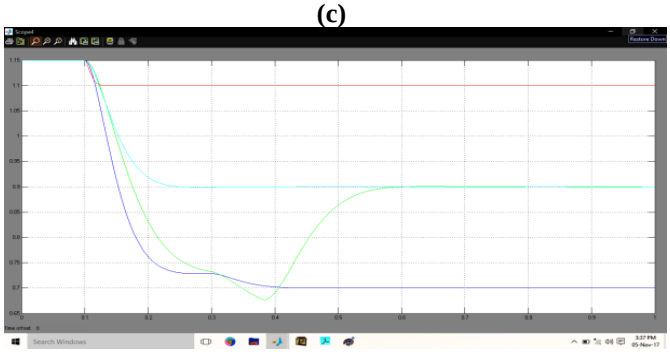

(d)

Fig.10: Results for Case 6. (a) System frequency. (b) Gain in Scheme #2 and the proposed scheme.(c) P_{WPP}. (d) Rotor speed.

Figure 10 shows the results for Case 6, which is identical to Case 5 except for a subsequent disturbance 0.2 s after the first disturbance. Thus, during the early stage of an event, the results before 0.3 s are the same as they are in Case 5. At the instant of the second event, ωr in Scheme #1 is slightly higher than it is in the proposed scheme; in addition, kadap is set to 11. When the second event occurs, Scheme #1 releases more output power than the proposed scheme (see Fig. 10(c)). Note that kadap increases up to 16.9 because the magnitude of df/dt increases due to the second disturbance; afterward, kadap keeps decreasing with declining df/dt and ωr and converges to 7.1. Thus, ωr in Scheme #1 reaches ωmin at 0.3 s, which is earlier than it is in Case 5. At this instant, an SFD occurs, thus the second FN is lower than it is in the proposed scheme by 0.17 Hz. ωr in the proposed scheme converges to 0.74 p.u. by reducing kadap, and thereby it ensures stable operation of a DFIG. The above results demonstrate that the proposed scheme successfully prevents wr from reaching ωmin by modifying the control gain with df/dt and ωr even when a subsequent event occurs after a significant wind speed reduction.

IV. CONCLUSION

An adaptive STFS scheme of a DFIG that can improve the frequency-supporting capability while ensuring stable operation. In the proposed scheme, the adaptive gain is modified with the ROCOF and rotor speed. During the early stage of an event, the gain is set to high; until the FN, the gain decreases with the ROCOF and rotor speed; after the FN, the gain decreases only with the rotor speed. The various simulation results demonstrate that the proposed scheme improves the FN under various wind conditions and disturbances while ensuring stable operation of a DFIG, even if the wind speed decreases and/or a consecutive event occurs. The advantages of the proposed scheme are that it can support the frequency by releasing a large amount of KE during the initial stage of an event. In addition, it can retain the KE available for a consecutive disturbance by reducing the output power after the FN. Further, it can ensure stable operation of a DFIG by reducing the control gain with the rotor speed even if the wind speed significantly decreases while supporting the frequency. Therefore, it can help stabilize the frequency under various wind conditions and disturbances, thereby providing a solution to ancillary services of STFS from a WTG.

V. REFERENCES

[1] H. Bevrani, Robust Power System Frequency Control. New York, NY, USA: Springer-Verlag, 2009.
[2] J. Machowski, J. W. Bialek, and J. R. Bumby, Power System Dynamic: Stability and Control. 2nd ed. Hoboken, NJ, USA: Wiley, 2011.
[3] C.Concordia, L.H. Fink, and G. Poullikkas, "Load shedding on an isolated system," IEEE Trans. Power Syst., vol. 10, no. 3, pp. 1467–1472, Aug. 1995.
[4] J.Kabouris and F.D.Kanellos, "Impacts of large-scale wind penetration on designing and operation of electric power systems," IEEE Trans. Sustain. Energy, vol. 1, no. 2, pp. 107–114, Jul. 2010.
[5] M. Liserre, R. Cardenas, M. Molinas, and J. Rodriguez, "Overview of multi-MW wind turbines and wind parks," IEEE Trans. Ind. Electron., vol. 58, no. 4, pp. 1081–1095, Apr. 2011.
[6] A. Mullane and M. O'Malley, "The inertial response of inductionmachine- based wind turbines," IEEE Trans. Power Syst., vol. 20, no. 3, pp. 1496–1503, Aug. 2005.
[7] Y. Xue and N. Tai, "Review of contribution to frequency control through variable speed wind turbine," Renew. Energy, vol. 36, no. 6, pp. 1671–1677, Jun. 2011.
[8] J.B.Ekanayake andN. Jenkins, "Comparison of the response of doubly fed and fixed-speed induction generator wind turbines to changes in network frequency," IEEE Trans. Energy Convers., vol. 19, no. 4, pp. 800–802, Dec. 2004.
[9] J. Morren, J. Pierik, and S. W. H. de Haan, "Inertial response of variable speed wind turbines," Elect. Power Syst. Res., vol. 76, no. 11, pp. 980–987, Jul. 2006.
[10] J. Morren, S.W. H. de Haan,W. L.Kling, and J.A. Ferreira, "Wind turbines emulating inertia and supporting primary frequency control," IEEE Trans. Power Syst., vol. 21, no. 1, pp. 433–434, Feb. 2006.

Author's Profile:

C.Nagamani currently persuing her M.Tech in Electrical Power Systems from SITS in Kadapa Affiliated to JNT University, Anantapuramu. She had done her B.Tech degree from MKITW, Rajampet in 2014 and his field of interest includes Power Systems**.**

K.Vijaya Kamal has 1 year of experience in teaching in Graduate and Post Graduate level and He Presently working as Assistant Professor in department of EEE in SITS, Kadapa, AP, India.

G.Venkata Suresh Babu has 14 years of experience in teaching in Graduate and Post Graduate level and he presently working as Associate Professor and HOD of EEE department in SITS, Kadapa, AP, India.